

The Variable Binding Modes of Phenylbis(pyrid-2-ylmethyl)phosphane and Bis(pyrid-2-ylmethyl) Phenylphosphonite with Ag^I and Cu^I

Fernando Hung-Low,^[a] Amanda Renz,^[a] and Kevin K. Klausmeyer*^[a]

Keywords: N,P ligands / Silver / Metal-metal interactions / Coordination modes

A series of new bridging phosphane and phosphonite structures forming three- and six-membered rings with the metal centers were synthesized and characterized. The resulting compounds of phenylbis(pyrid-2-ylmethyl)phosphane (**1**) with the silver(I) salts of trifluoroacetate (tfa⁻), tetrafluoroborate (BF₄⁻), and trifluoromethanesulfonate (OTf⁻), and copper tetrakis(acetonitrile) hexafluorophosphate (PF₆⁻) shows the flexibility of the ligand by displaying different coordination modes associated with the electronic and structural characteristics of the corresponding anion. Accordingly, ligand **1** in these complexes displays two different binding modes. With Agtfa and AgBF₄ compounds **3** and **4** are obtained where the ligand chelates to two silver atoms that exhibit normal Ag–Ag contacts in the range of 2.9 Å. When AgOTf or Cu(NCCH₃)₄PF₆ are used, one molecule of **1** bridges the

metal centers through a phosphorus atom while another is terminally bound. This induces short M–M distances of 2.6871 and 2.568 Å for **5** and **6**, respectively. Similarly, the coordination behavior of the heterofunctional bis(pyrid-2-ylmethyl) phenylphosphonite ligand (**2**) is reported with Cu(NCCH₃)₄PF₆ (**7**) and AgBF₄ (**8**) to form two novel discrete molecules. In these complexes **2** coordinates through the P and N atoms, with the difference that in **7** the O atom of one of the carbinol arms is also bound to the Cu. Elemental analysis, variable-temperature multinuclear NMR spectroscopy, single-crystal X-ray diffraction, and low-temperature luminescence studies were carried out to fully characterize the compounds.

(© Wiley-VCH Verlag GmbH & Co. KGaA, 69451 Weinheim, Germany, 2009)

Introduction

The coordination chemistry of bifunctional pyridylphosphane ligands has been explored for many years. A wide variety of ligands containing a pyridyl functionality in conjunction with phosphorus in the form of phosphanes, phosphinites, phosphonites, phosphates and phosphazoles have been synthesized and studied.^[1–4] Complexes synthesized with these ligands have exhibited catalytic^[1,5–7] and luminescence properties, as well as being useful in the construction of extended structures.^[8–11]

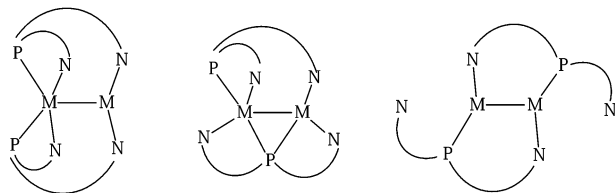
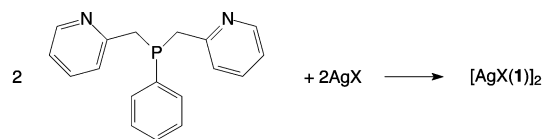
We have mainly been interested in synthesizing pyridyl-containing phosphinites and phosphonites where the pyridyl is attached at either the 3- or 4-position which precludes the formation of discrete chelating structures.^[8,10,12] More recently we have begun studies on derivatives that are attached to the phosphorus in the 2 position.^[11,13] Accordingly, the flexible tritopic ligands phenylbis(pyrid-2-ylmethyl)phosphane (**1**) and bis(pyrid-2-ylmethyl) phenylphosphonite (**2**), also known as hemilabile ligands because of the presence of a soft phosphane moiety combined with a

harder functionality^[14,15] were synthesized and their coordination ability toward Ag^I and Cu^I salts was studied. Several reports show **1** acting as a face capping ligand in octahedral metal complexes, as well as being a ligand suitable for use in catalysis.^[6,16,17] The flexible nature of the ligand implies the possibility of additional coordination modes, for instance with metals that require angles larger than the 90° of the octahedral environment. The close proximity of the binding functionalities can lead to the ligand bridging across two metal centers when chelation becomes difficult. Tertiary phosphanes which bridge two metal centers are a relatively recent discovery. Examples have been reported for several late transition metals including Pt^{II}, Pd^{II},^[18–20] Rh^I,^[21,22] Cu^I,^[23,24] and most recently Ag^I.^[25,26] In the case of Cu and Ag a very sterically constrained phosphazole was used as the bridging ligand. On the other hand, **2** (see Scheme 2) has been recently described^[6] and the catalytic ability of its Ni⁺² complex to oligomerize ethylene was studied. X-ray data for metal complexes of this ligand have yet to be reported. The X-ray structure of complexes of **2** would prove informative since the added chain length imparted by the OCH₂ linker could allow for additional coordination varieties.

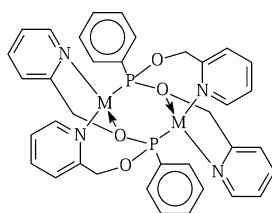
In this paper we demonstrate how with the very flexible ligand **1** different conformations can be achieved supporting Ag–Ag and Cu–Cu interactions (Scheme 1). Also shown is that with the larger **2** (Scheme 2) the added O functionality leads to an unusual N–O chelate to Cu^I.

[a] Department of Chemistry and Biochemistry, Baylor University, Waco, TX 76798, USA
Fax: +1-254-710-4272
E-mail: Kevin_Klausmeyer@baylor.edu

Supporting information for this article is available on the WWW under <http://dx.doi.org/10.1002/ejic.200900296>.



Scheme 1. Reaction of AgX with **1** and observed binding modes of the ligand.



Phenylbis(pyrid-2-ylmethyl)phosphane	1
Bis(pyrid-2-ylmethyl) Phenylphosphonite	2
[Ag _{tfa} (1) ₂]	3
[AgBF ₄ (1) ₂]	4
[AgOTf(1) ₂]	5
[CuPF ₆ (1) ₂]	6
[CuPF ₆ (2) ₂]	7
[AgBF ₄ (2) ₂]	8

Scheme 2. Binding modes of ligand **2** (M = Ag⁺ or Cu⁺).

Results and Discussion

Synthesis

Phosphane **1** was synthesized with modifications of a previously reported procedure^[16] where the percent yield of the ligand was improved by using temperatures of -41 and -84 °C during the reaction. Two crucial steps of the reaction were identified to be responsible for the formation of several unidentified phosphane oxide byproducts, as well as the overall yield of the final compound. Special care must be taken during the formation of the (pyridylmethyl)lithium and its addition to the phosphorus halide as high temperatures and rapid addition rates result in poor yield and purity of the ligand. Additionally, hexane extractions of the crude product allowed isolation of the ligand as a white powder with $>98\%$ purity, as opposed to the creamy yellow oil previously reported.^[6,16] Pure **1** is thermally stable, and can be preserved for a period up to 6 months under an inert atmosphere. Phenylphosphonite **2** is made by a procedure similar to that reported for the synthesis of bis(pyrid-3-ylmethyl) phenylphosphonite,^[9] and the singly substituted de-

rivative.^[27] Ligand **2** is considerably more sensitive than its singly substituted counterpart, decomposing more readily in solution at room temperature. The purified compound is a pale yellow oil that readily oxidizes and hydrolyzes in air, and decomposes when exposed to heat or light. The ligand can be preserved under inert atmosphere and at -35 °C for a period of only three days, upon which time hexane extractions are required to separate **2** from its decomposition products. ¹H and ³¹P NMR spectra of **1** and **2** in CDCl₃ and CD₃CN respectively, verify the formation of the ligands, with phosphorus singlets at -13.73 for **1** and 160.06 ppm for **2**, which are in the region expected for phosphane and phosphonite ligands.

The compounds **3–8** were synthesized by direct reaction in a 1:1 ratio of the corresponding ligand with the appropriate silver(I) salt (tfa⁻, BF₄⁻, or OTf⁻) or [Cu(CH₃CN)₄][PF₆] under ambient conditions. The complexes of **1** were shown to be stable at room temperature, surviving exposure to air with little sign of decomposition, provided the complexes are shielded from light. The Cu compound **6**, has proved to be the most stable among these, as it can be indefinitely stored in air at room temperature. Compounds of ligand **2** decompose very quickly even under inert conditions in a period of two or three days, and more rapidly in solution. Decomposition of the silver complexes is characterized by a change to a brown color from the initial white solids, and the Cu compound **7** from white to a green or blue solid, which is indicative of oxidation of the copper centers. The range of structural motifs observed in crystal structures **3**, **4**, **5**, and **8** is demonstrative of the ease with which the silver(I) cation varies its coordination sphere to accept the number of donors required of it. This coordinative property allows for a better study of the functionality characteristics of the ligands as they exhibit different coordination modes throughout the metal complexes. Coordination numbers from 3 to 5 are seen in the silver(I) compounds, while the copper(I) complexes are 4- and 5-coordinate. This versatility in coordination gives rise to several distorted geometries such as T-shaped (**4**), tetrahedral (**3**, **5**, **7**, and **8**), capped tetrahedral (**5**), and trigonal bipyramidal (**4**). The different coordination modes reported for the compounds of **1** are affected by the counterion's extent of interaction with the metal center. All of the compounds presented here were determined to be dimeric in the crystalline state with 1:1 ligand to metal ratios. Ligand **2** binds in a similar way to Ag and Cu, but with the added interaction of the O with the metal in the Cu complex to achieve a tetrahedral geometry. Counterion effects are not observed in the coordination of **2** to silver, as a reaction with Ag_{tfa} formed a crystal structure analogous to that reported for **8**. All metal complexes reported herein were characterized by X-ray diffraction, NMR spectroscopy, fluorescence, and elemental analysis, except for compound **8**, where its instability at room temperature gives inconsistent elemental analysis results. Accordingly, formation of **8** was also confirmed by HRMS results. For all of the compounds reported here attempts were made to alter the ligand to metal ratio, in each case the 1:1 ratio was obtained upon crystallization.

Description of the Crystal Structures

The equimolar reaction of **1** with Agtfa gives complex **3** as shown in Figure 1. The X-ray diffraction study shows an inversion center relating the two halves of the complex. Compound **3** displays a symmetric bridging interaction of the ligands to the metal centers, resulting in a distorted tetrahedral geometry for the silver, with the angles ranging between 79.7(2)° to 117.2(5)°. The Ag–Ag distance is 2.9499(4) Å and the Ag1–N2 distance is 2.786(2) Å, well beyond normal bonding distance. In this case the strongly binding of the tfa anion completes the coordination sphere such that the binding of the additional pyridine is unfavored due to the steric demands of chelation. There is also likely a stabilizing effect from the Ag–Ag interaction which also allows the pyridyl to remain free.

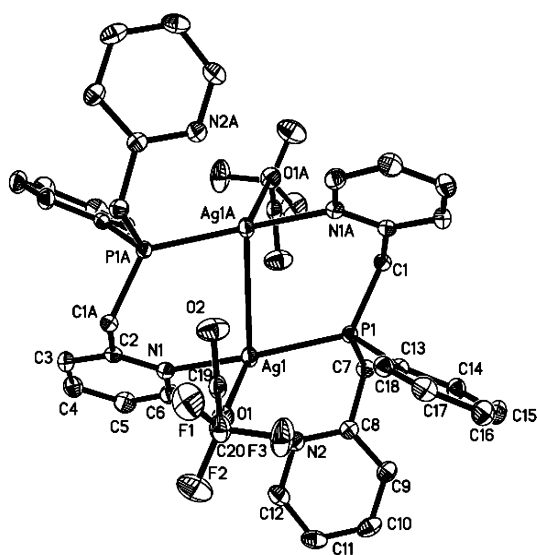


Figure 1. Thermal ellipsoid plot of **3** with an atomic numbering scheme. Ellipsoids are shown at the 50% level. Hydrogen atoms and a CH₂Cl₂ solvent molecule have been removed for clarity.

The X-ray crystal structure of compound **4**, which results from the equimolar reaction of **1** with AgBF₄, shows an unsymmetrical binding of the ligand. The phosphorus of both ligands as well as a pyridyl arm chelate to the same silver (Ag2) resulting in a distorted trigonal bipyramidal geometry [P1–Ag2–P2 154.54(3)°], as shown in Figure 2. Ag1 has two pyridyl moieties ligated, giving a slightly distorted T-shaped geometry, where the angles are N3–Ag1–Ag2 86.11(7)°, N2–Ag1–Ag2 83.18(7)° and N3–Ag1–N2 168.86(10)°.

The metal–metal distance in **4** is found to be 2.9922(4) Å, which is in the typical range for Ag–Ag distances. The Ag–P bonds also display typical values for both compounds **3** and **4**, while the Ag1–N bonds for **4** are noticeably shortened ≈ 2.160 Å, due to the low coordination number (Table 1).

The reaction of **1** with AgOTf (1:1 ratio) in CH₂Cl₂ at room temperature gives the compound whose crystal structure is shown in Figure 3, in which the two metal centers are bridged by a phosphorus from one ligand while the P

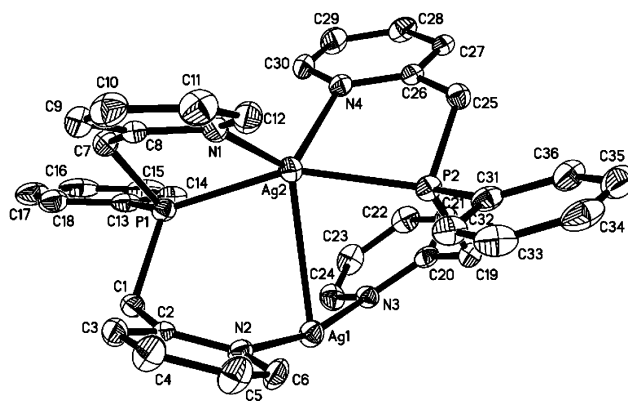


Figure 2. Thermal ellipsoid plot (50% level) of the cationic portion of **4** with an atomic numbering scheme. Hydrogen atoms have been removed for clarity.

Table 1. Selected bond lengths and angles for compounds **3–5**.

3			
Ag(1)–N(1)	2.275(2)	Ag(1)–P(1)	2.3960(7)
Ag(1)–O(1)	2.4091(19)	Ag(1)–Ag(1)#1	2.9499(4)
N(1)–Ag(1)–P(1)	145.25(6)	N(1)–Ag(1)–O(1)	95.06(7)
P(1)–Ag(1)–O(1)	116.35(5)	N(1)–Ag(1)–Ag(1)#1	99.70(5)
P(1)–Ag(1)–Ag(1)#1	79.716(17)	O(1)–Ag(1)–Ag(1)#1	117.15(5)
4			
Ag(1)–N(3)	2.160(3)	Ag(1)–N(2)	2.164(3)
Ag(1)–Ag(2)	2.9922(4)	Ag(2)–N(4)	2.395(3)
Ag(2)–N(1)	2.411(3)	Ag(2)–P(1)	2.4589(9)
Ag(2)–P(2)	2.4613(9)		
N(3)–Ag(1)–N(2)	168.86(10)	N(3)–Ag(1)–Ag(2)	86.11(7)
N(2)–Ag(1)–Ag(2)	83.18(7)	N(4)–Ag(2)–N(1)	122.94(10)
N(4)–Ag(2)–P(1)	114.32(7)	N(1)–Ag(2)–P(1)	76.84(7)
N(4)–Ag(2)–P(2)	77.68(7)	N(1)–Ag(2)–P(2)	116.71(7)
P(1)–Ag(2)–P(2)	154.54(3)	N(4)–Ag(2)–Ag(1)	120.25(7)
N(1)–Ag(2)–Ag(1)	116.80(7)	P(1)–Ag(2)–Ag(1)	78.26(2)
P(2)–Ag(2)–Ag(1)	76.35(2)		
5			
Ag(1)–N(1)	2.251(5)	Ag(1)–P(2)	2.4096(14)
Ag(1)–N(4)	2.533(5)	Ag(1)–P(1)	2.5947(14)
Ag(1)–Ag(2)	2.6871(6)	Ag(2)–N(3)	2.260(5)
Ag(2)–N(2)	2.277(5)	Ag(2)–O(1)	2.555(4)
Ag(2)–P(1)	2.5681(14)		
N(1)–Ag(1)–P(2)	131.09(12)	N(1)–Ag(1)–N(4)	90.78(17)
P(2)–Ag(1)–N(4)	77.06(12)	N(1)–Ag(1)–P(1)	80.69(12)
P(2)–Ag(1)–P(1)	147.42(5)	N(4)–Ag(1)–P(1)	114.42(12)
N(1)–Ag(1)–Ag(2)	138.70(12)	P(2)–Ag(1)–Ag(2)	89.50(4)
N(4)–Ag(1)–Ag(2)	108.26(11)	P(1)–Ag(1)–Ag(2)	58.15(3)
N(3)–Ag(2)–N(2)	108.36(16)	N(3)–Ag(2)–O(1)	96.75(15)
N(2)–Ag(2)–O(1)	111.35(15)	N(3)–Ag(2)–P(1)	145.84(12)
N(2)–Ag(2)–P(1)	80.97(12)	O(1)–Ag(2)–P(1)	110.58(10)
N(3)–Ag(2)–Ag(1)	102.18(11)	N(2)–Ag(2)–Ag(1)	139.56(11)
O(1)–Ag(2)–Ag(1)	90.23(10)	P(1)–Ag(2)–Ag(1)	59.12(3)

from the other ligand is bound terminally. The metal–metal distance in **5**, 2.6871(6) Å, is found to be among the shortest reported, for example the bis{μ₂-2-[bis(trimethylsilyl)methyl]pyridyl}disilver(I) (2.654 Å),^[28] the bis{[μ₂-1,3-diphenyltriazenido-*N,N'*]silver} (2.669 Å)^[29] and the bis[μ₂-

N,N'-bis(trimethylsilyl)benzenediamidinato-*N,N'*]disilver (2.665 Å).^[30] The Ag1–P1 and Ag2–P1 bonds are nearly identical, differing by only 0.027 Å. Both Ag1 and Ag2 are pentacoordinate with the environment about Ag1 being AgP₂N₂ and the environment about Ag2 being AgPN₂O due to the coordinating triflate. The pyridyl rings of the bridging phosphane ligand approach a coplanar conformation, as evidenced by the P1–C1–C2–N1 and the P1–C7–C8–N2 torsion angles of 36.1(5)° and 33.5(5)° respectively. The comparable torsion angles for the P2 ligand are 70.9(5) and 50.9(6)°. P2 is 3.592(1) Å from Ag2, and the Ag1–P2 bond is typical at 2.410(11) Å, as is the pyridyl–Ag distance between N2–Ag2, 2.257(5) Å. The pyridyl–Ag distance between N1–Ag1 displays an unusually long bond of 2.538(4) Å; this could be attributed to the orientation of the pyridyl ring which does not point directly at the Ag emphasizing the steric stress in the complex.

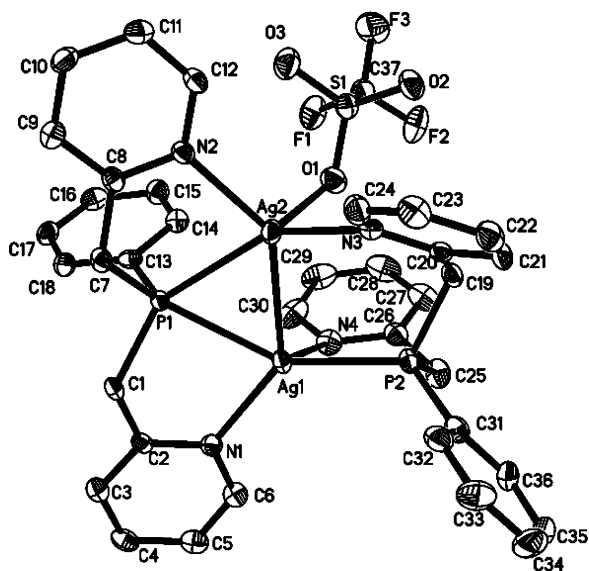


Figure 3. Thermal ellipsoid plot (50% level) of the cationic portion of **5** with an atomic numbering scheme. Hydrogen atoms, one triflate anion and one solvent CH₂Cl₂ molecule have been removed for clarity.

An X-ray diffraction study revealed that the Cu^I complex **6**, obtained from **1** and an equimolar amount of [Cu(CH₃CN)₄][PF₆], has the structure shown in the Figure 4, in which the two metal centers are bridged by a phosphane donor, and the second ligand is a terminal bound bridging ligand, very similar to **5**.

The different metal coordination environments in the crystal structure of **6** once again show the ability of the ligand to coordinate either terminally (P1), or bridging (P2). The conformation of the ligand in this complex seems to be quite sensitive to the affinity of Cu^I to achieve tetrahedral angles, where geometric effects contribute either to the bridging or terminal bond interactions. The metal–metal distance in **6** [2.488 (12) Å] is the shortest reported for a copper complex bridged by phosphane. The first Cu...Cu-bridged phosphane compound was reported with the 2,5-di(pyrid-2-yl)phosphole and a metal–metal distance of

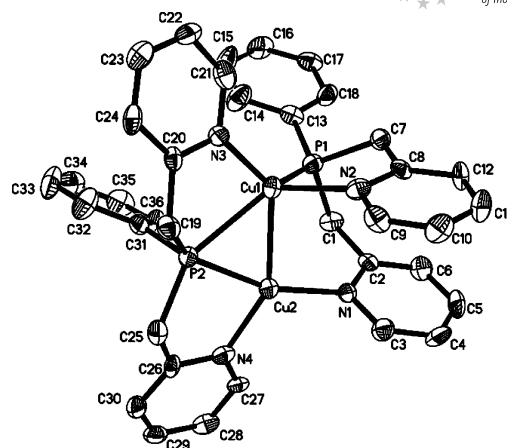


Figure 4. Thermal ellipsoid plot (50% level) of the cationic portion of **6** with an atomic numbering scheme. Hydrogen atoms and the two PF₆[−] anions have been removed for clarity.

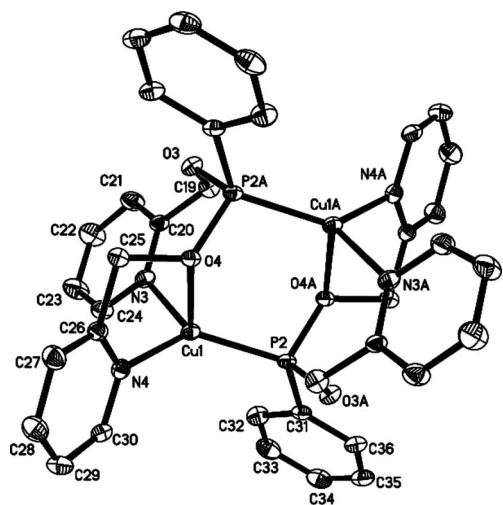
2.568 Å,^[23] the phosphole is a more rigid ligand hence the bridging interaction is likely promoted more by the constrained geometry of the ligand. It should be noted that the Cu1–P2 and Cu2–P2 interactions are not symmetric, as in **5**, differing by 0.243 Å (Table 2). The Cu1 atom has a distorted capped tetrahedral geometry due to the bridging interaction that distorts the symmetry of the angles, ranging from 53.28(2)° to 131.23(16)°. Cu2 has a distorted tetrahedral geometry due to both the chelating behavior of one of the ligands and the bridging interaction presented through P2, ranging the angles from 53.28(5)° to 159.20(17)°. The terminally bound ligand shows a close pyridyl π separation of 3.653 Å and an angle of 17.22(26)°. This favorable π-stacking interaction may help account for the close proximity of Cu1 to Cu2, allowing for the opposing phosphane to undergo the 3-centered bridge. The P1–Cu2 distance is 3.376(5) Å, well beyond bonding distance. The Cu1–P2 bond is typical at 2.254(2) Å, as are the pyridyl–Cu distances of 2.092(6) and 1.949(5) Å for N2–Cu1 and N1–Cu2, respectively.

The crystal structure of compound **7** contains two coppers and two molecules of ligand **2**. The ligand bridges the two copper centers to create a symmetric and discrete molecule (Figure 5). The Cu environment is a distorted tetrahedron. In order to achieve this geometry, the O atom from one of the carbinol arms is ligated to the Cu. This unusual bonding sequence between the metal center and the ligand has been previously reported with Fe,^[31] Ru,^[32,33] Sn,^[34] Li,^[35] Na^[36–38] and K.^[39] Each of the previously reported structures had smaller, symmetric ligands, and none of them were di- or tritopic. The Cu1–O4 bond has a distance of 2.399(2) Å, and there is no Cu–Cu interaction, the distance being 3.820 Å. The hexagonal ring at the center of structure created by the P–O–Cu progression is oriented in a chair conformation. A reaction mixture of a 2:3 metal to ligand ratio produced only crystals of **7**.

The X-ray crystal structure of compound **8** reveals a slightly alternate conformation of the ligand. The two nitrogens are seen chelating the Ag center, while the phosphorus

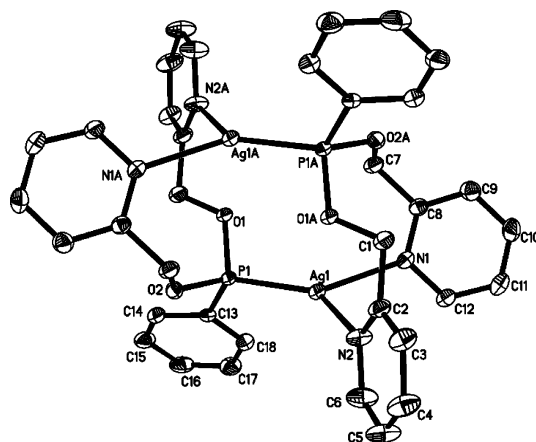
Table 2. Selected bond lengths and angles for **6–8**.

6			
Cu(1)–N(3)	1.994(5)	Cu(1)–N(2)	2.092(6)
Cu(1)–P(1)	2.254(2)	Cu(1)–Cu(2)	2.4882(12)
Cu(1)–P(2)	2.497(2)	Cu(2)–N(1)	1.949(5)
Cu(2)–N(4)	2.030(5)	Cu(2)–P(2)	2.235(2)
N(3)–Cu(1)–N(2)	110.4(2)	N(3)–Cu(1)–P(1)	126.96(16)
N(2)–Cu(1)–P(1)	85.30(16)	N(3)–Cu(1)–Cu(2)	134.34(16)
N(2)–Cu(1)–Cu(2)	96.95(15)	P(1)–Cu(1)–Cu(2)	89.97(6)
N(3)–Cu(1)–P(2)	81.56(17)	N(2)–Cu(1)–P(2)	131.23(16)
P(1)–Cu(1)–P(2)	126.02(7)	Cu(2)–Cu(1)–P(2)	53.28(5)
N(1)–Cu(2)–N(4)	112.8(2)	N(1)–Cu(2)–P(2)	159.20(17)
N(4)–Cu(2)–P(2)	87.58(17)	N(1)–Cu(2)–Cu(1)	96.93(16)
N(4)–Cu(2)–Cu(1)	149.28(17)		
7			
Cu(1)–N(3)	2.020(3)	Cu(1)–N(4)	2.027(3)
Cu(1)–P(2)	2.1549(9)	Cu(1)–O(4)	2.399(2)
Cu(2)–N(2)	2.029(3)	Cu(2)–N(1)	2.033(3)
Cu(2)–P(1)	2.1594(9)	Cu(2)–O(1)	2.413(2)
N(3)–Cu(1)–N(4)	105.73(11)	N(3)–Cu(1)–P(2)	122.71(9)
N(4)–Cu(1)–P(2)	129.64(8)	N(3)–Cu(1)–O(4)	99.70(10)
N(4)–Cu(1)–O(4)	74.94(10)	P(2)–Cu(1)–O(4)	106.93(6)
N(2)–Cu(2)–N(1)	104.81(11)	N(2)–Cu(2)–P(1)	125.40(8)
N(1)–Cu(2)–P(1)	128.30(8)	N(2)–Cu(2)–O(1)	97.33(9)
N(1)–Cu(2)–O(1)	74.41(10)	P(1)–Cu(2)–O(1)	107.25(6)
8			
Ag(1)–N(2)	2.317(3)	Ag(1)–N(1)	2.336(3)
Ag(1)–P(1)	2.3460(10)		
N(2)–Ag(1)–N(1)	86.47(12)	N(2)–Ag(1)–P(1)	135.90(9)
N(1)–Ag(1)–P(1)	137.28(8)		

Figure 5. Thermal ellipsoid plot (50% level) of the cationic portion of **7** with an atomic numbering scheme. Hydrogen atoms and the two PF_6^- anions have been removed for clarity.

bridges to the opposing Ag producing a discrete dimer (Figure 6). The trigonal planar environments of the metal centers exhibit angles ranging from 86.47° to 137.28°. The varying of the metal from Cu to Ag eliminated the strong tetrahedral affinity resulting in both Ag atoms being three-coordinate. The Ag–N and Ag–P distances range from

2.317 to 2.346 Å and fall within reported values. The packing structure of compound **8** shows long range interactions holding the BF_4^- anion in place by CH–F and Ag–F interactions with distances of 2.258 and 2.727 Å respectively.

Figure 6. Thermal ellipsoid plot (50% level) of the cationic portion of **8** with an atomic numbering scheme. Hydrogen atoms, the two BF_4^- anions and one solvent CH_2Cl_2 molecule have been removed for clarity.

NMR Spectroscopy

The ^1H and ^{31}P NMR spectra of all compounds were collected in different solvents due to the solubility of each compound. The ^1H NMR spectra of compounds **3–6** are, as expected, generally similar, as well as between **7** and **8**. ^{31}P NMR spectra were recorded at room and low temperatures to observe the dissociation of the M–P bonds, the lability of the M–P bond even at low temperatures precluded observation of the coupling of the two isotopes of Ag to P. The room temperature ^{31}P NMR spectra of both **3** and **4** showed a defined phosphorus resonance at $\delta = 8.7$ and 9.9 ppm respectively. Upon cooling to -45°C , the signal for **3** begins to show coupling with Ag, giving a resonance at $\delta = 11.2$ ppm, while **4** shows similar behavior at $\delta = 11.2$ ppm. At room temperature the ^{31}P NMR spectrum of **5** shows again a broad phosphorus signal at $\delta = 11.8$ ppm, which indicates that in solution the P is not bridging the Ag atoms, and may instead be chelating the metal centers. Upon cooling to -45°C , this broad signal splits into an unsymmetrical resonance at $\delta = 12.0$ ppm indicating that in solution the structure likely is different than that reported by X-ray diffraction. Possibly, even at low temperatures the P1–Ag2 interaction is dissociated thus resulting in a conformation similar to that reported for **3**, which explains the similar spectra observed for **3** and **5**. The ^{31}P spectrum of **6** shows a broad phosphorus resonance at $\delta = -15.5$ ppm, indicating fluxional Cu–P bonding in solution. Upon cooling to -45°C this broad signal splits into two singlets at -31.2 and -2.2 ppm, resulting from two separate phosphorus environments present at low temperature, corresponding to the terminal and bound bridging phosphorus, respectively. As a result, the low-temperature ^{31}P NMR of **6**

agrees with the crystal structure reported for the compound. The ^{31}P NMR spectra of **7** and **8** show analogous signals, as expected, with a singlet at $\delta = 134.9$ and 142.2 ppm respectively, as the crystal structures display a similar structural motif. The variable temperature ^{31}P NMR also showed singlet signals for both complexes, indicative of a fast equilibrium even at low temperatures.

Photoluminescence

Photoluminescence experiments were conducted on complexes **3–8**. The low-temperature solution luminescence spectra were collected to give a general representation of what the solid state spectra would be (Figure S1). The resemblance of the excitation spectra of compounds **3–6** with that of free **1** suggests that the luminescent behavior of these complexes is initiated by a ligand-based absorption, which then decays by means of ligand-to-metal charge transfer. A clear dependence is observed between the intensities in which energy is absorbed, and the type of coordination metal–ligand encountered in the complex. Excitation maxima of all compounds are presented in Table 3 along with the local emission maxima. The emission spectra of the various compounds cover a range of the spectrum with local maxima spanning approximately 100 nm. Analyzing only the spectra of the three silver–ligand compounds, we find that the order in intensities increase in the following sequence: $[\text{AgBF}_4(\mathbf{1})_2]_2 > [\text{Ag}(\text{tfa})(\mathbf{1})_2]_2 > [\text{AgOTf}(\mathbf{1})_2]_2$. The luminescence properties of the compounds of ligand **2** (**7** and **8**) were also tested, however, their rapid decomposition under ambient conditions precluded the collection of the spectra, even when the corresponding solutions were prepared under inert atmosphere.

Table 3. Luminescence spectroscopic data for compounds **3–6** at 77 K and 1×10^{-4} M in CH_3CN .

Compound	Excitation λ_{max} /nm	Emission λ_{max} /nm
3	315	441, 455, 466
4	301	462
5	314	438
6	327	473, 491, 500, 512

Conclusions

Herein we have demonstrated that several coordination environments and coordination numbers can be formed with Ag^{I} and Cu^{I} salts, being controlled either by variations in counterion or coordinative ability of the ligand. The series **3–5** displays the flexibility of **1** to bind to Ag^{I} . In each case the preferred chelating angle is greater than 90° for which the ligand is ideally suited. This results in both bridging and chelating by the ligand to two metal centers. In addition, a very flexible tertiary phosphane is shown with two Ag^{I} centers forming a very short argentophilic interaction. A similar result is obtained by reaction of **1** with $\text{Cu}(\text{NCCH}_3)_4\text{PF}_6$, as the ligand bridges and chelates two coppers and induces a short cuprophilic interaction. Ligand

2 is also shown to be versatile as it is seen to act as a tridentate and tetradentate ligand, forming a stable six-member ring with the metal centers.

Future work in our group encompasses the design and synthesis of more hemilabile pyridyl-containing phosphanes and phosphinites. Additionally, we are also actively pursuing the oxidation of ligand **1** to its oxide derivatives, as the incorporation of one or more oxygen moieties, combined with the demonstrated flexibility of the ligand, can exhibit an interesting coordinative behaviour to different transition metals and lanthanide starting materials.

Experimental Section

General Remarks: All experiments were carried out under a nitrogen atmosphere, using a Schlenk line and standard Schlenk techniques. Glassware was dried at 120°C for several hours prior to use. Solvents were distilled under nitrogen from the appropriate drying agent immediately before use. ^1H and ^{31}P NMR spectrum were recorded at 499.78 and 202.32 MHz respectively, on a Varian 500 MHz spectrometer. Fluorescence spectra were recorded on an Instruments S. A. Inc. model Fluoromax-2 spectrometer using band pathways of 2.5 nm for both excitation and emission and are presented uncorrected. Elemental analyses were performed by Atlantic Microlabs Inc., Norcross, Georgia. High resolution mass spectra (HRMS) were obtained in the Baylor University Mass Spectrometry Core Facility on a Thermo Scientific LTQ Orbitrap Discovery using +ESI.

Materials: Dichlorophenylphosphane was purchased from Aldrich Chemical and used as received. Triethylamine was purchased from Aldrich and was purged with nitrogen before use. 2-pyridylcarbinol was purchased from Alfa Aesar and used as received. Silver salts were purchased from Strem Chemicals Inc. and stored in an inert-atmosphere glovebox. $[\text{Cu}(\text{CH}_3\text{CN})_4][\text{PF}_6]$ was prepared according to published procedures.^[40]

General Synthesis: General procedures for the synthesis of compounds **3–8** involve the addition of a 5 mL solution of the corresponding ligand **1** or **2** in either CH_3CN or CH_2Cl_2 , to a stirred solution of the appropriate salt in 5 mL of solvent. The mixtures were then allowed to stir for 10 min and then dried in vacuo to leave white or off-white powders. The flasks containing the silver compounds were shielded from light with aluminum foil to prevent photodecomposition. Colorless blocks of the four silver compounds were obtained by slow diffusion of hexane into a CH_2Cl_2 solution of **3**, **4**, **5**, and **7** at 5°C . Crystals of compounds **6** and **8** were grown by layering ether over acetonitrile solutions at 5°C . The amounts of reagents used, yields, and spectroscopic data are presented below as well as any modifications to the general synthetic procedure. Percent yields are based upon the amount of the corresponding silver or copper salt used.

Phenylbis(pyrid-2-ylmethyl)phosphane (1): This compound was synthesized by addition of *n*-butyllithium (17 mmol, 5.86 mL, 2.9 M in hexane) over a period of 10 min to 2-picoline (17 mmol, 1.67 mL) in dry THF (20 mL) at -41°C . The mixture was stirred for 1 h, then added to a solution of dichlorophenylphosphane (3.0 g, 17 mmol) in dry THF (20 mL) at -84°C over a period of 30 min. Degassed water (25 mL) was then added over 10 min and the mixture stirred for 30 min. The product was obtained by first extracting with 0.3 N HCl(aq), then neutralizing with aqueous NaHCO_3 solution, and a final extraction with dichloromethane. The solvent and any unreacted 2-picoline were removed under vacuum (oil pump)

resulting in a yellow oil. The yield of crude product was 81%. Purification of the product was carried out by several extractions with hexane which resulted in a white solid in 70% yield based on 2-picoline. ^1H NMR (CD_3Cl , 298 K): δ = 3.41 (q, 4 H, CH_2), 7.02 (m, 4 H, aromatic), 7.33 (m, 3 H, aromatic), 7.49 (m, 4 H, aromatic), 8.52 (m, 2 H, aromatic) ppm. ^{31}P NMR (CDCl_3 , 298 K): δ = -13.7 (s) ppm.

Bis(pyrid-2-ylmethyl) Phenylphosphonite (2): In a nitrogen-purged addition funnel, 1.39 mL of degassed triethylamine (10 mmol) was added via syringe to a stirred solution of pyridine-2-methanol (1.09 g, 10 mmol) in toluene (20 mL) at room temperature. The solution was cooled to 0 °C and shielded from light with aluminum foil. A solution of dichlorophenylphosphane (0.896 g, 5 mmol) in toluene (20 mL) was then added dropwise over 10 min. The solution was stirred for 1 h, and warmed to room temperature, followed by stirring for an additional 30 min. The resultant mixture was filtered through Celite. The triethylammonium chloride salt was washed with an additional 5 mL of cold toluene, and the solvent was removed from the yellow liquid at reduced pressure to leave a yellow oil. The oil was then extracted with 100 mL of hexane to leave **2** as a pale yellow oil in 84% yield (1.36 g, 4.36 mmol). ^1H NMR (CH_3CN , 298 K): δ = 5.01 (m, 4 H, CH_2), 7.09 (t, 3 H, aromatic), 7.66 (m, 7 H, aromatic), 8.43 (d, 3 H, aromatic) ppm. ^{31}P NMR (CD_3CN , 298 K): δ = 160.1 (s) ppm.

Synthesis of [Ag₂(1)]₂ (3): This reaction used **1** (0.116 g, 0.398 mmol) in CH_3CN (5 mL) added to a stirred solution of Agtfa (0.880 g, 0.398 mmol) in CH_3CN (5 mL) to leave a fluffy off-white solid. The compound was re-crystallized upon drying in 48% (0.190 g, 0.185 mmol) yield. ^1H NMR (CDCl_3 , 298 K): δ = 4.05 (m, 8 H, CH_2), 7.31 (m, 14 H, aromatic), 7.68 (m, 4 H, aromatic), 7.85 (m, 4 H, aromatic), 8.47 (d, 4 H, aromatic) ppm. ^{31}P NMR [$(\text{CD}_3)_2\text{CO}$, 298 K]: δ = 8.7, s; [$(\text{CD}_3)_2\text{CO}$, 238 K]: δ = 11.2, t ppm. $\text{C}_{41}\text{H}_{36}\text{Ag}_2\text{Cl}_2\text{F}_6\text{N}_4\text{O}_4\text{P}_2$ (1111.54): calcd. C 44.31, H 3.26, N 5.04; found C 43.82, H 3.33, N 4.84.

Synthesis of [AgBF₄(1)]₂ (4): The reaction was done in a 1:1 ratio of **1** (0.117 g, 0.396 mmol) in CH_3CN (5 mL) to AgBF_4 (0.077 g,

0.396 mmol) in CH_3CN (5 mL). Solvent was removed in vacuo to obtain an off-white powder. This was then re-dissolved in a small amount of CH_2Cl_2 and precipitated with hexane, repeating until compound **4** was obtained as a white powder upon drying in 51% (0.180 g, 0.202 mmol) yield. ^1H NMR (CDCl_3 , 298 K): δ = 4.35 (m, 8 H, CH_2), 7.58 (m, 14 H, aromatic), 7.98 (m, 8 H, aromatic), 8.60 (d, 4 H, aromatic) ppm. ^{31}P NMR [$(\text{CD}_3)_2\text{CO}$, 298 K]: δ = 9.9, s; [$(\text{CD}_3)_2\text{CO}$, 231 K]: δ = 11.2 (d) ppm. $\text{C}_{37}\text{H}_{36}\text{Ag}_2\text{B}_2\text{Cl}_2\text{F}_8\text{N}_4\text{P}_2$ (1058.91): calcd. C 41.97, H 3.43, N 5.29; found C 42.21, H 3.48, N 5.47.

Synthesis of [AgOTf(1)]₂ (5): To a stirred solution of AgOTf (0.109 g, 0.399 mmol) in CH_3CN (5 mL) was added **1** (0.116 g, 0.399 mmol) in CH_3CN (5 mL). The compound was re-crystallized upon drying in 49% (0.210 g, 0.194 mmol) yield. ^1H NMR (CDCl_3 , 298 K): δ = 4.31 (m, 8 H, CH_2), 7.32 (m, 6 H, aromatic), 7.49 (m, 8 H, aromatic), 7.85 (t, 4 H, aromatic), 7.96 (m, 4 H, aromatic), 8.45 (d, 4 H, aromatic) ppm. ^{31}P NMR [$(\text{CD}_3)_2\text{CO}$, 298 K]: δ = 11.8, s; [$(\text{CD}_3)_2\text{CO}$, 298 K]: δ = 12.1, t ppm. $\text{C}_{39}\text{H}_{36}\text{Ag}_2\text{Cl}_2\text{F}_6\text{N}_4\text{O}_6\text{P}_2\text{S}_2$ (1169.39): calcd. C 39.58, H 3.07, N 5.23; found C 40.13, H 3.16, N 4.91.

Synthesis of [CuPF₆(1)]₂ (6): A solution of **1** (0.116 g, 0.399 mmol) in CH_3CN (5 mL) was added to $[\text{Cu}(\text{CH}_3\text{CN})_4][\text{PF}_6]$ (0.149 g, 0.399 mmol) dissolved in CH_3CN (5 mL). Compound **6** was obtained as a white powder upon drying in 85% (0.170 g, 0.170 mmol) yield. ^1H NMR (CDCl_3 , 298 K): δ = 3.83 (m, 4 H, CH_2), 7.47 (m, 11 H, aromatic), 8.21 (m, 2 H, aromatic) ppm. ^{31}P NMR [$(\text{CD}_3)_2\text{CO}$, 298 K]: δ = -15.5, s; [$(\text{CD}_3)_2\text{CO}$, 228 K]: δ = -31.2 (s, br), -2.2 (s) ppm. $\text{C}_{36}\text{H}_{34}\text{Cu}_2\text{F}_{12}\text{N}_4\text{P}_4$ (1001.65): calcd. C 43.17, H 3.42, N 5.59; found C 43.12, H 3.31, N 5.62.

Synthesis of [CuPF₆(2)]₂ (7): To a stirred solution of $[\text{Cu}(\text{CH}_3\text{CN})_4][\text{PF}_6]$ (0.111 g, 0.297 mmol) in CH_2Cl_2 (5 mL), was added to **2** (0.097 g, 0.299 mmol) in CH_2Cl_2 (5 mL). This solution was stirred for 5 min, and then 45 mL of ether were added. Upon stirring for 10 min a white precipitate formed. The colorless solvent was removed via cannula, and the residual solvent was removed in vacuo to leave a white solid, **7**, in 81% (0.278 g, 0.358 mmol) yield. ^1H

Table 4. Crystallographic data for compounds 3–5.

	3	4	5
Empirical formula	$\text{C}_{42}\text{H}_{38}\text{Ag}_2\text{Cl}_4\text{F}_4\text{N}_4\text{O}_4\text{P}_2$	$\text{C}_{36}\text{H}_{34}\text{Ag}_2\text{B}_2\text{F}_8\text{N}_4\text{P}_2$	$\text{C}_{39}\text{H}_{36}\text{Ag}_2\text{Cl}_2\text{F}_6\text{N}_4\text{O}_6\text{P}_2\text{S}_2$
Formula mass	1196.24	973.97	1183.42
$a/\text{\AA}$	9.9151(8)	10.4667(8)	9.7199(7)
$b/\text{\AA}$	10.5773(9)	13.3392(8)	13.9612(10)
$c/\text{\AA}$	11.8770(10)	14.1342(11)	16.5420(11)
$\alpha/^\circ$	81.442(4)	102.466(2)	79.481(3)
$\beta/^\circ$	79.351(4)	104.341(2)	80.510(3)
$\gamma/^\circ$	75.428(4)	93.595(2)	82.583(3)
$V/\text{\AA}^3$	1177.90(17)	1852.7(2)	2165.5(3)
Z	1	2	2
Crystal system	triclinic	triclinic	triclinic
Space group	$P\bar{1}$	$P\bar{1}$	$P\bar{1}$
T/K	110(2)	110(2)	110(2)
$D_{\text{calcd.}}/\text{g cm}^{-3}$	1.686	1.746	1.815
μ/mm^{-1}	1.195	1.218	1.276
$2\theta_{\text{max.}}/^\circ$	26.37	25.00	25.00
Reflections measured	23421	17285	37239
Reflections used (R_{int})	4759 (0.0290)	7388 (0.0350)	7565 (0.0423)
Restraints/parameters	0/289	0/487	0/568
$R_1 [I > 2\sigma(I)]$	0.0307	0.0353	0.0525
$wR_2 [I > 2\sigma(I)]$	0.0800	0.0742	0.1517
$R(F_o^2)$ (all data)	0.0331	0.0506	0.0592
$R_w(F_o^2)$ (all data)	0.0816	0.0824	0.1593
GOF on F^2	1.036	1.017	1.010

Table 5. Crystallographic data for compounds **6** through **8**.

	6	7	8
Empirical formula	C ₃₆ H ₃₄ Cu ₂ F ₁₂ N ₄ P ₄	C ₃₇ H ₃₆ Cl ₂ Cu ₂ F ₁₂ N ₄ O ₄ P ₄	C ₃₈ H ₃₈ Ag ₂ B ₂ Cl ₄ F ₈ N ₄ O ₄ P ₂
Formula mass	1001.63	1150.56	1207.82
<i>a</i> / Å	9.559(19)	11.8810(7)	9.5811(13)
<i>b</i> / Å	25.281(5)	15.0617(9)	16.958(2)
<i>c</i> / Å	16.763(3)	16.3276(10)	13.9024(18)
<i>α</i> / °	90	67.705(3)	90
<i>β</i> / °	101.892(6)	74.534(3)	101.357(6)
<i>γ</i> / °	90	68.830(3)	90
<i>V</i> / Å ³	3962.8(13)	2492.3(3)	2214.6(5)
<i>Z</i>	4	2	2
Crystal system	monoclinic	triclinic	monoclinic
Space group	<i>P</i> 2 ₁ / <i>n</i>	<i>P</i> $\bar{1}$	<i>P</i> 2 ₁ / <i>n</i>
<i>T</i> / K	110(2)	110(2)	110(2)
<i>D</i> _{calcd.} / g cm ⁻³	1.679	1.533	1.811
<i>μ</i> / mm ⁻¹	1.326	1.174	1.278
2 θ _{max.} / °	25.00	26.53	26.51
Reflections measured	22722	74451	24112
Reflections used (<i>R</i> _{int})	8017 (0.1376)	10282 (0.0312)	4545 (0.0278)
Restraints/parameters	0/523	0/587	0/289
<i>R</i> ₁ [<i>I</i> > 2 σ (<i>I</i>)]	0.0756	0.0556	0.0386
<i>wR</i> ₂ [<i>I</i> > 2 σ (<i>I</i>)]	0.0906	0.1422	0.1129
<i>R</i> (<i>F</i> _o ²) (all data)	0.1860	0.0672	0.0420
<i>R</i> _w (<i>F</i> _o ²) (all data)	0.1154	0.1490	0.1167
GOF on <i>F</i> ²	1.002	1.063	1.055

NMR (CD₃CN, 298 K): δ = 5.04 (d, 4 H, CH₂), 7.35 (d, 9 H, aromatic), 7.41 (s, 2 H, aromatic), 8.22 (s, 2 H, aromatic) ppm. ³¹P NMR (CD₃CN, 298 K): δ = 134.9 (s, br); (CD₃CN, 225 K): δ = 130.3 (s) ppm. C₃₆H₃₄Cu₂N₄O₄P₂ (775.73): calcd. C 40.58, H 3.22, N 5.26; found C 40.85, H 3.13, N 5.36.

Synthesis of [AgBF₄(2)]₂ (8**):** To a stirred solution of AgBF₄ (0.0577 g, 0.300 mmol) in CH₃CN (5 mL) was added **2** (0.099 g, 0.306 mmol) in CH₃CN (5 mL). The resulting solution was allowed to stir for 15 min and then dried in vacuo to leave a pale yellow oil. The oil was then dissolved in 5 mL of CH₂Cl₂, and precipitated with 50 mL of hexane. The colorless solution was removed via cannula, and the solvent removed in vacuo to leave a white solid, **8**, in 75%. (0.105 g, 0.115 mmol) yield. ¹H NMR (CD₃CN, 298 K): δ = 5.08 (d, 4 H, CH₂), 7.50 (m, 4 H, aromatic), 7.67 (m, 3 H, aromatic), 7.82 (m, 2 H, aromatic), 7.96 (m, 2 H, aromatic), 8.64 (m, 2 H, aromatic) ppm. ³¹P NMR (CD₃CN, 298 K): δ = 142.2 (s); (CD₃CN, 243 K): δ = 140.2 (s) ppm. +ESI-HRMS for [C₁₈H₁₇Ag-N₂O₂P]⁺ calcd. 431.0079 *m/z*; found 431.0065 *m/z*.

X-Ray Crystallographic Study: Crystallographic data were collected on crystals with dimensions 0.281 × 0.201 × 0.188 mm for **3**, 0.209 × 0.153 × 0.102 mm for **4**, 0.340 × 0.210 × 0.170 mm for **5**, 0.094 × 0.062 × 0.055 mm for **6**, 0.335 × 0.242 × 0.145 mm for **7** and 0.350 × 0.280 × 0.180 mm for **8**. Data were collected at 110 K on a Bruker X8 Apex using Mo-*K* α radiation (λ = 0.71073 Å). The structures were solved by direct methods and refined by full-matrix least-squares refinement on *F*². Multi-scan absorption corrections were applied using the program SADABS.^[41,42] Crystal data are presented in Tables 4 and 5, and selected interatomic distances and angles are given in Tables 1 and 2. All of the data were processed using the Bruker AXS SHELXTL software, version 6.10.^[22,43] Unless otherwise noted, all non-hydrogen atoms were refined anisotropically and hydrogen atoms were placed in calculated positions.

Supporting Information (see also the footnote on the first page of this article): Low-temperature luminescence spectra of complexes **3–6**.

Acknowledgments

This research was supported by funds provided by grant from the Robert A. Welch Foundation (AA-1508). The Bruker X8 APEX diffractometer was purchased with funds received from the National Science Foundation Major Research Instrumentation Program Grant CHE-0321214

- [1] P. Espinet, K. Soulantica, *Coord. Chem. Rev.* **1999**, *193*, 499–556.
- [2] R. Meijboom, R. J. Bowen, S. J. Berners-Price, *Coord. Chem. Rev.* **2009**, *253*, 325–342.
- [3] G. R. Newkome, *Chem. Rev.* **1993**, *93*, 2067–2089.
- [4] S. E. Durrant, M. B. Smith, S. H. Dale, S. J. Coles, M. B. Hursthouse, M. E. Light, *Inorg. Chim. Acta* **2006**, *359*, 2980–2988.
- [5] P. A. Aguirre, C. A. Lagos, S. A. Moya, C. Zuniga, C. Vera-Oyarce, E. Sola, G. Peris, J. C. Bayon, *Dalton Trans.* **2007**, 5419–5426.
- [6] A. Kermagoret, F. Tomicki, P. Braunstein, *Dalton Trans.* **2008**, 2945–2955.
- [7] F. Speiser, P. Braunstein, L. Saussine, *Dalton Trans.* **2004**, 1539–1545.
- [8] K. K. Klausmeyer, R. P. Feazell, J. H. Reibenspies, *Inorg. Chem.* **2004**, *43*, 1130–1136.
- [9] R. P. Feazell, C. E. Carson, K. K. Klausmeyer, *Inorg. Chem.* **2005**, *44*, 996–1005.
- [10] R. P. Feazell, C. E. Carson, K. K. Klausmeyer, *Acta Crystallogr., Sect. C* **2004**, *60*, m598–m600.
- [11] F. Hung-Low, K. K. Klausmeyer, *Inorg. Chim. Acta* **2008**, *361*, 1298–1310.
- [12] F. Hung-Low, K. K. Klausmeyer, J. B. Gary, *Inorg. Chim. Acta* **2009**, *362*, 426–436.
- [13] F. Hung-Low, K. K. Klausmeyer, *Acta Crystallogr., Sect. E.* **2007**, *63*, m1931.
- [14] A. Cingolani, E. Di Nicola, D. Martini, C. Pettinari, B. W. Skelton, A. H. White, *Inorg. Chim. Acta* **2006**, *359*, 2183–2193.
- [15] M. P. Felicissimo, A. A. Batista, A. G. Ferreira, J. Ellena, E. E. Castellano, *Polyhedron* **2005**, *24*, 1063–1070.

- [16] E. Lindner, H. Rauleder, W. Hiller, *Z. Naturforsch.* **1983**, *38*, 1130–1136.
- [17] K. K. Klausmeyer, F. Hung, *Acta Crystallogr., Sect. E.* **2006**, *62*, m2415–m2416.
- [18] F. Leca, M. Sauthier, V. Deborde, L. Toupet, R. Reau, *Chem. Eur. J.* **2003**, *9*, 3785–3795.
- [19] P. Braunstein, N. Boag, *Angew. Chem. Int. Ed.* **2001**, *40*, 2427–2433.
- [20] M. Sauthier, B. Le Guennic, V. Deborde, L. Toupet, J. Halet, R. Réau, *Angew. Chem. Int. Ed.* **2001**, *40*, 228–231.
- [21] H. Werner, *Angew. Chem. Int. Ed.* **2004**, *43*, 938–954.
- [22] T. Pechman, C. D. Brandt, H. Werner, *Angew. Chem. Int. Ed.* **2000**, *39*, 3909–3911.
- [23] F. Leca, C. Lescop, E. Rodriguez-Sanz, K. Coatuas, J. Halet, R. Reau, *Angew. Chem. Int. Ed.* **2005**, *44*, 4362–4365.
- [24] B. Nohra, E. Rodriguez-Sanz, C. Lescop, R. Reau, *Chem. Eur. J.* **2008**, *14*, 3391–3403.
- [25] S. Welsch, C. Lescop, M. Scheer, R. Reau, *Inorg. Chem.* **2008**, *47*, 8592–8594.
- [26] S. Welsch, B. Nohra, E. V. Peresypkina, C. Lescop, M. Scheer, R. Réau, *Chem. Eur. J.* **2009**, *15*, 4685–4703.
- [27] R. J. van Haaren, C. J. M. Drujven, G. P. F. van Strijdonck, H. Oevering, J. N. H. Reek, P. C. J. Kamer, P. W. N. M. van Leeuwen, *J. Chem. Soc., Dalton Trans.* **2000**, 1549–1554.
- [28] R. I. Papasergio, C. L. Raston, A. H. White, *J. Chem. Soc., Chem. Commun.* **1984**, *9*, 612–613.
- [29] M. Horner, A. G. Pedroso, J. Beck, J. Strahle, *B. Chem. Sci.* **1996**, *51*, 686–690.
- [30] D. Fenske, G. Baum, A. Zinn, K. Dehnicke, *B. Chem. Sci.* **1990**, *45*, 1273–1278.
- [31] D. Bucholz, G. Huttner, W. Imhof, *J. Organomet. Chem.* **1990**, *388*, 307–320.
- [32] T. Koyama, Y. Koide, K. Matsumoto, *Inorg. Chem.* **1999**, *38*, 3241–3243.
- [33] S. G. Bott, J. C. Wang, M. G. Richmond, *J. Chem. Crystallogr.* **1999**, *29*, 587–595.
- [34] K. Kawamura, H. Nakazawa, K. Miyoshi, *Organometallics* **1999**, *18*, 4785–4794.
- [35] J. Powell, A. Kuksis, C. J. May, S. C. Nyburg, S. J. Smith, *J. Am. Chem. Soc.* **1981**, *103*, 5941–5943.
- [36] K. Matsumoto, Y. Sano, *Inorg. Chem.* **1997**, *36*, 4405–4407.
- [37] J. Powell, A. Lough, F. Wang, *Organometallics* **1992**, *11*, 2289–2295.
- [38] J. Powell, K. S. Ng, W. W. Ng, S. C. Nyburg, *J. Organomet. Chem.* **1983**, *243*, C1–C4.
- [39] A. S. C. Chan, H.-S. Shieh, J. R. Hill, *J. Organomet. Chem.* **1985**, *279*, 171–179.
- [40] G. J. Kubas, *Inorg. Synth.* **1979**, *19*, 90–92.
- [41] G. M. Sheldrick, *SHELXTL* (v. 6.10), Madison, WI, USA, **2000**.
- [42] *APEX 2* (v. 2.0) and *SAINTPPLUS* (v. 6.25), Bruker, Madison, WI, USA, **2003**.
- [43] G. M. Sheldrick, *SHELXS97* and *SHELXL97*, University of Göttingen, Germany, **1997**.

Received: March 30, 2009
Published Online: May 26, 2009